

# Water in Local Free Volumes of Polyimides: A Positron Lifetime Study

G. Dlubek,<sup>\*,†</sup> R. Buchhold,<sup>‡</sup> Ch. Hübner,<sup>§</sup> and A. Nakladal<sup>‡</sup>

ITA Institut für innovative Technologien GmbH, Köthen, Aussenstelle Halle, D-06124 Halle, Germany; Edvard-Grieg-Weg 8, Technische Universität Dresden, Institut für Festkörperelektronik, D-01062 Dresden, Germany; and Martin-Luther-Universität Halle-Wittenberg, Fachbereich Physik, D-06099 Halle/S, Germany

Received September 1, 1998; Revised Manuscript Received January 4, 1999

**ABSTRACT:** Positron annihilation lifetime (PAL) spectroscopy was used to study the effect of water uptake on the free volume in 6FDA-ODA polyimide (PI2566, DuPont). Orthopositronium (o-Ps) lifetime ( $\tau_3$ ) and intensity ( $I_3$ ) data were analyzed assuming a Gaussian size distribution of preexisting (excess free volume) holes and further assuming that holes occupied by water molecules would not be detected in the measurement. When exposed to humidity, both the mean hole volume and the number of holes not occupied by water molecules decrease with increasing relative humidity, as indicated by decreasing  $\tau_3$  and  $I_3$ . Our PAL results correlated with humidity-induced mass uptake and volume expansion support a model according to which water absorption in polyimides occurs in two stages. At relative humidities smaller than about 30%, water is absorbed mostly in large, preexisting holes, with each hole typically occupied by a single water molecule. At larger humidities, an increasing fraction of the sorbed water molecules will occupy sites other than preexisting empty holes. A multiple occupation of larger holes by water molecules is discussed as a possible mechanism.

## Introduction

Owing to their superior mechanical and dielectric properties, coupled with excellent thermal stability and chemical resistance, polyimides have found widespread application as gas separation membranes and as insulating layers in microelectronic device fabrication.<sup>1,2</sup> A major drawback of these polymers is their hygroscopic nature which results in the absorption of up to 5% moisture under ordinary environmental conditions. The moisture absorption leads to swelling of the material, thus degrading its electrical properties. Several authors have investigated the transport of moisture in polyimide films,<sup>3,4</sup> but the exact mechanisms that govern humidity-induced water uptake and diffusion of water molecules within the material are still unclear. It is generally believed that both sorption and swelling behavior are closely related to the free-volume properties of the polyimide.

Positron annihilation lifetime (PAL) spectroscopy is a well-established and very sensitive technique for probing sub-nanometer-sized local free volumes in solids.<sup>5–8</sup> In molecular materials such as polymers, a fraction of the injected positrons will form a bound state called positronium (Ps).<sup>9</sup> The Ps appears either as a parapositronium (p-Ps, singlet spin state) or as an orthopositronium (o-Ps, triplet spin state), with a relative abundance of 1:3. In a vacuum, an o-Ps has a relatively long lifetime of 142 ns. When injected into matter, the positron of the Ps may collide with atoms or molecules and annihilate with an electron other than its bound partner and with opposite spin (pick-off annihilation). The result is a sharply reduced o-Ps lifetime depending on the collision frequency. Given a sufficiently large concentration of cavities in the sample, the Ps density is largely restricted to these open volumes, and the o-Ps pick-off lifetimes, which are

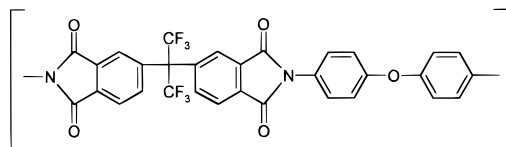


**Figure 1.** Chemical structure of polyimide PI2566 (6FDA-ODA).

typically in the nanosecond range, can be evaluated to estimate the size of the cavities.<sup>10–12</sup>

Several groups have recently reported on PAL studies on polyimides,<sup>13–21</sup> however, only a few papers focused on moisture absorption.<sup>20</sup> In the present work, we utilize PAL spectroscopy to investigate the effect of water sorption on the free volume in polyimide 6FDA-ODA. On the basis of the results, we estimate the number density of preexisting local free volumes (holes), their mean size, and their size distribution. In addition, we analyze our PAL results to draw conclusions regarding the nature of the hole-filling process as a function of relative humidity. PAL spectra are measured with a high statistical accuracy (total count of 16 M) and analyzed using the LIFSPECFIT<sup>22</sup> and MELT<sup>23</sup> routines. The effect of moisture exchange between the samples and our laboratory atmosphere during the measurements is controlled through repeated lifetime measurements. Finally, we compare the results from our PAL studies with results obtained from investigations on mass uptake and swelling.

## Experimental Section

**Sample Preparation.** Commercially available polyimide PI2566 (hexafluoropropane dianhydride-diaminodiphenyl ether, 6FDA-ODA, see Figure 1) of the Pyralin series from DuPont was chosen for this study. For most commercial applications, polymers such as PI2566 are typically prepared by spin-coating to form a thin, continuous layer on the substrate. The thickness of spin-coated films can be controlled by adjusting the spin speed; however, films with a thickness larger than about 50  $\mu\text{m}$  are often difficult to prepare. For conventional

<sup>†</sup> ITA Institut für innovative Technologien.

<sup>‡</sup> Technische Universität Dresden.

<sup>§</sup> Martin-Luther-Universität Halle.

PAL spectroscopy, thicker samples are desirable, since the positron absorption coefficients in polymers are rather small. Consequently, we have applied the following preparation techniques: (i) Water uptake and swelling behavior were studied on samples prepared by spin-coating, with layer thickness around 10  $\mu\text{m}$ , and 3 in. silicon wafers serving as the substrate.<sup>24,25</sup> (ii) For PAL spectroscopy, the polyimide precursor was cast into aluminum pans with a diameter of 8 mm and a height of 1.5 mm. The pans were filled repeatedly after solvent removal in order to achieve complete filling. (iii) Sample preparation has a significant effect on the polymer's morphology and material properties. Therefore, some samples were prepared by spin-coating using extremely low spin speeds to yield layers around 50–80  $\mu\text{m}$  thick. These samples were used to validate the PAL results obtained using samples prepared by casting.

After spin-coating or casting, samples were first dried (soft-baked) at a temperature of 90  $^{\circ}\text{C}$  to remove solvents. After solvent removal, samples were imidized (hard-baked) at a temperature of 400  $^{\circ}\text{C}$ , which was reached using a 2.5 K/min ramp and maintained for 1 h. After being hard-baked, samples were slowly cooled to room temperature. To confirm successful imidization, the chemical structure of the polyimide films was verified using FTIR spectroscopy.<sup>24</sup>

**Water Uptake and Swelling Investigations.** To determine the humidity-induced mass uptake in spin-coated polymer layers at different levels of humidity, a precision balance (BP210 from Sartorius, Inc.) based setup was used, with an accuracy of about 50  $\mu\text{g}$ . The climatic conditions inside the setup can be controlled between 15 and 35  $^{\circ}\text{C}$  and 0% and 85% relative humidity (RH). Atmospheres of different RH were obtained by controlled mixing of dry and moist air. In addition, experiments with wafer bending and spectral ellipsometry were carried out to determine the mechanical strain due to in-plane (ip) and out-of-plane (oop) swelling at different levels of humidity.<sup>24,25</sup> The results were used to calculate the volume expansion in the layer. Since diffusion times in thin polymer films are short, these measurements were carried out time-resolved under streaming air of controlled relative humidity (RH).

Samples processed by casting, on the other hand, typically have diffusion times in the range of several days or weeks, so time-resolved measurements are not feasible for these samples. Consequently, we have applied the following two approaches for cast samples: (i) Different samples of cast polyimide PI2566 were exposed to different levels of RH for 2 months. To maintain a precisely controlled relative humidity over long periods of time, saturated salt solutions were used.<sup>26</sup> The atmosphere above these solutions had RH of 11% (LiCl), 32% ( $\text{MgCl}_2$ ), 45% ( $\text{K}_2\text{CO}_3$ ), 55% (NaBr), 75% (NaCl), and 90% ( $\text{BaCl}_2$ ). Drying of polyimides was performed by exposing the samples in dry air of 70  $^{\circ}\text{C}$  for a period of 8 h. (ii) One of the cast samples, along with the thick, spin-coated PI2566 samples, was dried at 90  $^{\circ}\text{C}$  for several hours immediately before the positron experiments.

**Positron Lifetime Experiments.** All positron lifetime measurements were carried out at room temperature in ordinary laboratory atmosphere using a conventional fast–fast coincidence system<sup>5,9</sup> with a time resolution of 253 ps (full width at half-maximum, fwhm, of a Gaussian resolution function) and a channel width of 26.98 ps. For each experiment, two identical samples were sandwiched around a  $2 \times 10^6$  Bq positron source ( $^{22}\text{Na}$ ), which was prepared by evaporating carrier-free  $^{22}\text{NaCl}$  solution on an aluminum foil of 2  $\text{mg}/\text{cm}^2$  mass thickness. Four measurements, each lasting 2 h, were performed for each of the specimens and also for the reference material (p-type silicon). In preliminary inspections, the routine LIFSPECFIT was used to analyze each of the 2 h spectra (total count of 4 M) and evaluate the lifetime parameters and the position of the time zero. It was found that the time zeros of these spectra did not deviate by more than  $\pm 0.1$  channels. All spectra counts were summarized in a final spectrum with a total number of 16 million coincidence counts.

All of the lifetime spectra were analyzed using the routines LIFSPECFIT,<sup>22</sup> MELT,<sup>23</sup> and CONTIN-PALS2.<sup>27</sup> In the con-

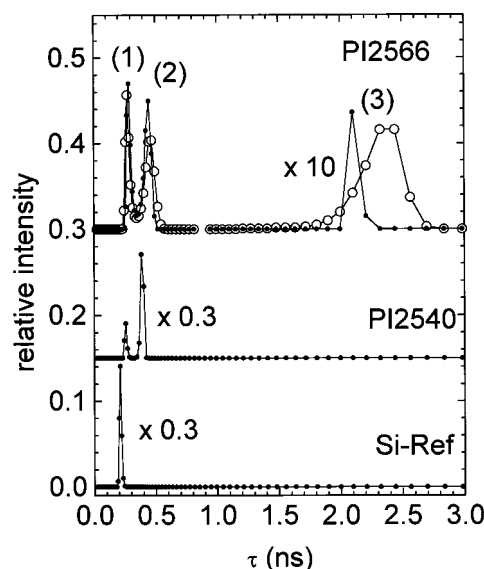


**Figure 2.** Positron lifetime distribution in the Si reference sample, a polyimide PI 2540 (Kapton) sample, and two polyimide PI2566 samples in the dry state (empty circles) and when exposed to 90% RH (filled circles). All distributions were obtained from the summarized 16 million count spectra using the MELT routine (entropy weight:  $2 \times 10^{-7}$ ).

ventional, discrete-term routine LIFSPECFIT, the positron lifetime spectrum is represented by a sum of negative exponentials,<sup>5,9</sup>

$$s(t) = \sum \frac{I_i}{\tau_i} \exp\left(-\frac{t}{\tau_i}\right) \quad (1)$$

where  $\tau_i$  is the positron lifetime in the  $i$ th state with a relative intensity  $I_i$ ,  $\sum I_i = 1$ . Analysis involves least-squares fitting of eq 1 during which the number of exponential terms has to be assumed, following convolution with the experimental resolution. In addition, a commonly used correction procedure for positrons annihilating within the source and the containing materials was applied (380 ps/2.5%, NaCl; 180 ps/1.5%, Al foil; and 2500 ps/0.4%, surface effects). Three components are resolved in the lifetime spectra of the dry and wet PI2566 samples.

The routine MELT (maximum entropy for lifetime analysis) assumes a continuous lifetime distribution

$$s(t) = \int \frac{I(\tau)}{\tau} \exp\left(-\frac{t}{\tau}\right) d\tau \quad (2)$$

and inverts  $s(t)$  into  $I(\tau)$  via a quantified maximum entropy method. Unlike the discrete-term analysis, it does not require any assumptions concerning the shape of  $I(\tau)$  or the number of components. However, a large total count of at least 10 million is typically necessary with MELT in order to obtain sufficient sensitivity to the shape of the distribution.<sup>23,28</sup>

## Results and Discussion

**The Positron Lifetime Parameters.** Typical lifetime distributions derived from the 16 million count spectra via the MELT routine are plotted in Figure 2. The Si reference shows only a single positron lifetime of 219 ps, which agrees well with values cited in the literature.<sup>5</sup> Three peaks are found in the lifetime distribution of polyimide PI2566. Each peak is associated with a characteristic lifetime  $\tau_i$  and an intensity  $I_i$  which can be estimated from the mass center of the peak and from the relative area below the peak, respectively. In dry polyimide PI2566, the lifetime parameters were estimated to be 270 ps/49.4%, 450 ps/46.2%, and 2280

ps/4.4%, which is in excellent agreement with the results from our LIFSPECFIT analysis. Results from the MELT analysis are very similar to those obtained using the CONTIN routine, except for greater sensitivity to the width of the peaks in the lifetime distribution.<sup>28</sup> Thus, only the results obtained with MELT will be discussed here.

When a positronium is formed in a polymer, three annihilation channels exist.<sup>5–12</sup> The short-lived p-Ps annihilates mainly by self-annihilation, with a lifetime of  $\tau_{p-Ps} = 125 \text{ ps}/\eta$ , where  $\eta$  describes the relaxation of Ps in matter, and 125 ps is the lifetime in a vacuum. For polyimides,  $\eta$  is not well-known<sup>9,29,30</sup> but is likely to be between 0.5 and 1. A second lifetime of  $\tau_{e+} = 300\text{--}400 \text{ ps}$  is due to free positron (not Ps) annihilation. Finally, a lifetime of a few nanoseconds is attributed to pick-off annihilation of the long-lived o-Ps ( $\tau_{o-Ps}$ ). Assuming that pick-off annihilation is the only o-Ps quenching process, it can be shown using statistical considerations that the intensities of the p-Ps and o-Ps components<sup>9</sup> are related as  $I_{p-Ps}/I_{o-Ps} = 1/3$ . Three characteristic lifetimes  $\tau_i$  are resolved in the PAL spectra of most polymers. They are usually attributed to p-Ps, free-positron, and o-Ps annihilation.<sup>5–12</sup> However, it is often observed that  $\tau_1$  is rather large compared with the expected  $\tau_{p-Ps}$  and in particular that the ratio  $I_1/I_3$  can be much larger than 1/3. In polyimide PI2566, this ratio was found to be abnormally large ( $I_1/I_3 = 11.2$ ). It has been shown recently<sup>28,31,32</sup> that these discrepancies can be explained, at least in part, by assuming a size distribution of the free-volume holes in amorphous polymers, which will result in a distribution of o-Ps lifetimes. Since an o-Ps lifetime distribution will cause an extra curvature in the lifetime spectra  $s(t)$ , as evident in a  $\log[s(t)]$  vs  $t$  plot, a discrete-term routine may overestimate the values of  $\tau_1$  and  $I_1$ .

However, our analysis of computer-generated lifetime spectra indicates that this effect is small when using the MELT or CONTIN routines.<sup>28</sup> From our computer simulations we have concluded that there may be another mechanism responsible for the observed discrepancies. It is known that, in addition to o-Ps, free positrons also annihilate inside free-volume holes in amorphous polymers.<sup>12,33</sup> We expect that a distribution of hole sizes and hole shapes will, in addition to an o-Ps lifetime distribution, also cause a positron lifetime distribution, centered around the mean value  $\tau_{e+}$ . If this distribution is particularly broad, both the MELT and the CONTIN analysis will be unable to exactly mirror the lifetime distribution. Instead of a broad distribution, these routines will extract two subpeaks.<sup>28</sup> Indeed, we have observed these two subpeaks in polyimide PI2540 (Kapton, see Figure 2) and in other polyimides where no Ps is formed. In polyimide PI2566, the lower of the two subpeaks in the  $e^+$  lifetime distribution overlaps with the small p-Ps lifetime peak, and thus cannot be separated from the distribution. Consequently, the individual lifetimes and intensities of the first and second components extracted from the lifetime spectra have no physical meaning, at least not in the case of the polyimide under investigation. Only the integral value  $I_1\tau_1 + I_2\tau_2$  agrees well with its physical origin  $I_{p-Ps}\tau_{p-Ps} + I_{e+}\tau_{e+}$ . The specifics of positron lifetime analysis are beyond the subject of this paper and will be discussed in greater detail elsewhere.<sup>28</sup>

From computer simulations we have also found that the o-Ps peak is located too far above the peaks

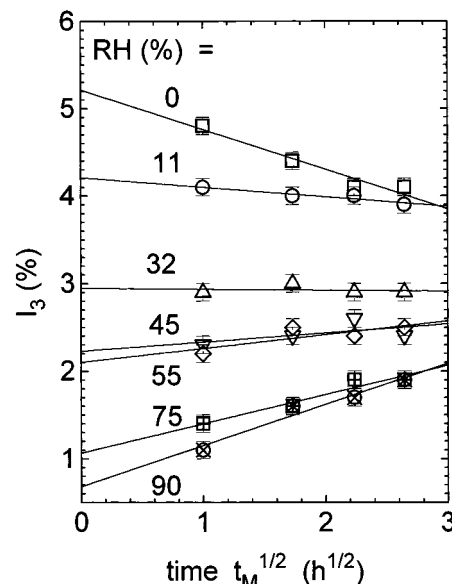


**Figure 3.** o-Ps intensity  $I_3$  as a function of the square root of measuring time  $\sqrt{t_M}$  in polyimide PI2566 samples exposed to different RH.

associated with the shorter-lived components, which indicates that the o-Ps peak is not affected by the lifetime distribution artifacts. Since the values for intensity  $I_3$  and lifetime  $\tau_3$  extracted from MELT and LIFSPECFIT show good agreement with the simulation results, we conclude that  $\tau_3 = \tau_{o-Ps}$  and  $I_3 = I_{o-Ps}$ . As can be seen in Figure 2, only the o-Ps annihilation process depends on the material properties. The mass center of the o-Ps peak  $\tau_3$ , its width, and its area  $I_3$  all decrease with increasing water uptake in the case of polyimide PI2566.

The parameters extracted for each polyimide PI2566 specimen from the 2 h PAL spectra typically change between the first and the fourth measurement. To reduce the statistical scattering in the extracted parameters, we have applied the routine LIFSPECFIT and fixed  $\tau_1$  to its average of 270 ps. In the case of samples equilibrated in an atmosphere of larger humidity the parameters  $I_3$ ,  $\tau_3$ , and  $I_3\tau_3$  increase over time, while in those exposed to smaller humidity the lifetime parameters decrease. Similar behavior was also reported by other authors.<sup>20</sup> We attribute the observed behavior to water desorption from the samples and water sorption into the samples during the measurement. Only those samples that are exposed to a humidity equal to that of the laboratory atmosphere ( $\sim 30\% \text{ RH}$ ,  $25^\circ \text{C}$ ) are in a steady-state condition during the measurement. This is illustrated in Figure 3 which plots the o-Ps intensity  $I_3$  as a function of the square root of measurement time,  $\sqrt{t_M}$ .  $I_3$  decreases or increases linearly with  $\sqrt{t_M}$ . Such behavior, typically observed in sorption and desorption curves of mass uptake,<sup>34,35</sup> serves as evidence for the validity of Fick's law of diffusion. PAL experiments show an enhanced sensitivity for surface-near regions in a sample, since the positron implantation profile follows a negative exponential,<sup>5</sup>  $\alpha \exp(-\alpha x)$  with  $\alpha = 58 \text{ cm}^{-1}$  for materials of mass density  $\rho = 1.4 \text{ g/cm}^3$ .

Figures 4–6 show the lifetime parameters  $I_3$ ,  $\tau_3$ , and  $I_3\tau_3$  for polyimide PI2566 samples exposed to ambient atmospheres of different humidity. For each of these parameters the results from the MELT analysis of the summarized (16 million total count) spectra are shown together with the results for the first (4 million count)



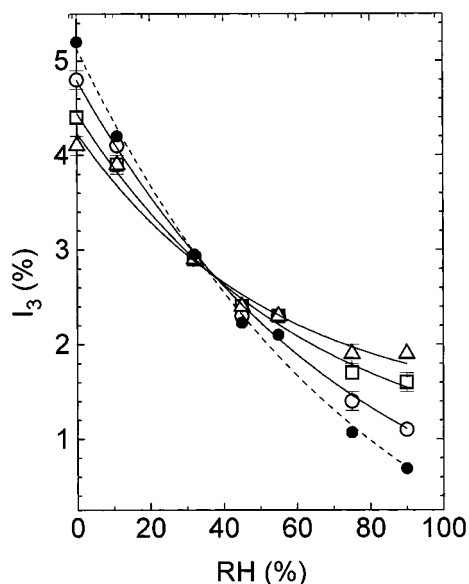


**Figure 4.** o-Ps intensity  $I_3$  as a function of RH in polyimide PI2566 samples exposed to different RH: empty squares, MELT analysis of summarized spectra (all other symbols: LIFSPECFIT analysis with  $\tau_1$  fixed to 270 ps); open circles, first measurements; open triangles, fourth measurements; filled circles, parameter extrapolated to  $t_M \rightarrow 0$ ; see Figure 2. The solid and dashed lines are least-squares fits of a negative exponential to the data points.

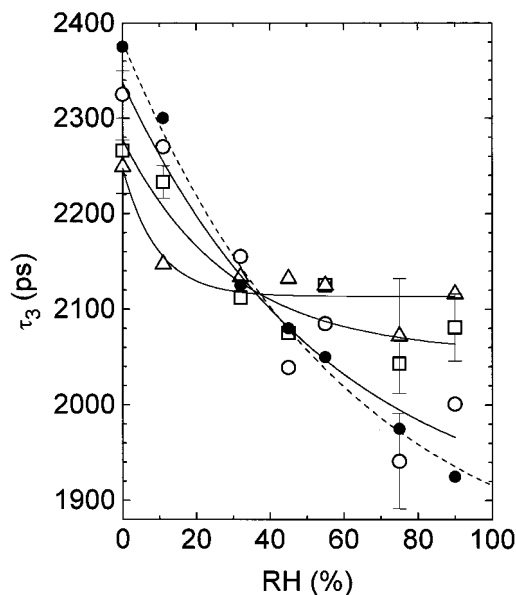
and fourth measurement, analyzed using the LIFSPECFIT routine and a fixed  $\tau_1 = 270$  ps. Also shown are results obtained by extrapolating the corresponding parameter to  $t_M \rightarrow 0$  (see Figure 3, for example). The plots show that all of the parameters  $I_3$ ,  $\tau_3$ , and  $I_3\tau_3$  decrease with increasing humidity. This behavior will be explained later as the filling of free volume holes by sorbed water molecules. Note that the curves plotted using data obtained for shorter  $t_M$  have a larger slope than those obtained for longer  $t_M$ .

Figure 6 shows the value  $I_3\tau_3$  and the "average lifetime of the first and second component",  $\tau(1,2)_{av}$ , which we define as

$$\tau(1,2)_{av} = \frac{I_1\tau_1 + I_2\tau_2}{I_1 + I_2} = \frac{I_{p-Ps}\tau_{p-Ps} + I_{e+}\tau_{e+}}{I_{p-Ps} + I_{e+}} \quad (3)$$

As discussed previously, this value corresponds to the average lifetime associated with the p-Ps and  $e^+$  annihilation (right-hand side of eq 3).  $\tau(1,2)_{av}$  decreases linearly from 361 ps in the dry state to 356 ps at 90% RH.  $\tau(1,2)_{av}$  may be corrected for p-Ps annihilation to obtain the  $e^+$  lifetimes. Assuming  $\tau_{p-Ps} = 150$  ps and  $I_{p-Ps} = I_3/3$ , the estimated positron lifetime  $\tau_{e+}$  changes from 365 to 357 ps with increasing humidity. Similarly to the decrease in  $\tau_3$ , this slight decrease in  $\tau_{e+}$  may be attributed to the hole filling by sorbed water molecules, in this case probed by free positrons. Similar relationships between the free positron and o-Ps lifetimes were also observed and reported by other authors.<sup>12,33</sup>

**Hole Filling Due to Sorbed Water Molecules in Polyimide PI2566.** Glassy polymers contain cavities or holes of atomic or molecular dimensions which are due to irregular molecular packing in the amorphous phase and are usually referred to as static and preexisting holes. The holes form an (excess) free volume which effects the thermal, the mechanical, and the relaxation properties of the polymer. It is believed that the



**Figure 5.** As Figure 3, but o-Ps lifetime  $\tau_3$ .

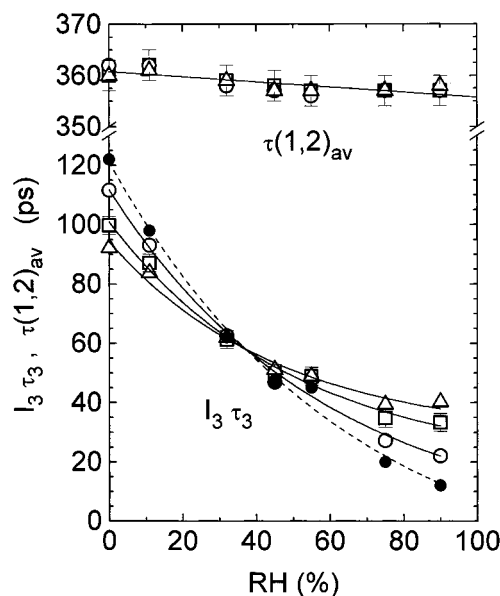


**Figure 6.** As Figure 3, but parameters  $I_3\tau_3$  and  $\tau(1,2)_{av}$  (see text).

transport of molecules, stemming from liquids or gases absorbed from the ambient atmosphere, occurs through these holes. The mean size of the holes can be estimated from the o-Ps lifetime<sup>10-12</sup>  $\tau_3$ . As a result of the repulsive exchange interaction between electrons from the Ps atoms and electrons from the macromolecules, the Ps population in amorphous polymers tends to be restricted to open spaces (holes). A simple model incorporating quantum-mechanical and empirical considerations provides an analytic expression relating the radius  $r$  of the hole (assumed to be spherical) to the observed o-Ps pick-off lifetime,

$$\tau_3 = \tau_{o-Ps} = 0.5 \left[ 1 - \frac{r}{r + \delta r} + \frac{1}{2\pi} \sin\left(\frac{2\pi r}{r + \delta r}\right) \right]^{-1} \quad (4)$$

The factor of 0.5 ns is the spin-averaged Ps annihilation lifetime which is also observed in densely packed molecular crystals.  $\delta r$  represents the depth of the penetration of the Ps wave function into the walls of

the hole which is modeled<sup>36</sup> by a square-well potential of infinite depth and radius  $r$ . A widely used value of  $\delta r = 0.166$  nm is obtained by fitting eq 4 to observed o-Ps lifetime of known mean hole radii in porous materials.<sup>10,11</sup> Using eq 4, the mean hole radius  $r_0$  can be extracted using either a single  $\tau_3$  obtained from discrete-term analysis or the mass center of the o-Ps lifetime distribution. Under particular circumstances a distribution of hole radii may be estimated from a distribution of o-Ps lifetimes<sup>37</sup> delivered by the MELT or CONTIN inversion techniques. We have estimated the mean hole volume  $v_0(\text{RH}) = 4\pi r_0^3/3$  using extrapolated  $\tau_3(t_M \rightarrow 0)$  values (Figure 5) and found that  $v_0$  decreases from  $v_0 = 0.134$  nm<sup>3</sup> ( $r_0 = 0.317$  nm) to 0.092 nm<sup>3</sup> (0.28 nm) when the relative humidity is increased from 0 to 90% (see Figure 10). As discussed earlier, the apparent decrease in the mean hole size can be attributed to the fact that with increasing humidity more and more holes are occupied by sorbed water molecules.

For a more detailed discussion including the effects of a hole size distribution, we shall follow the work of Kirchheim<sup>38,39</sup> (see also the literature<sup>40</sup>). Considerations by Bueche<sup>41</sup> based on the theory of fluctuations lead to a Gaussian size distribution of free volume holes,

$$n(v) = \frac{N_0}{\sigma_0 \sqrt{2\pi}} \exp\left(-\frac{(v - v_0)^2}{2\sigma_0^2}\right) \quad (5)$$

where  $N_0$  is the number density of holes,  $v_0$  the average hole size, and  $\sigma_0$  the width (standard deviation) of the distribution. The fractional free volume  $f$  is given by

$$f = \int_0^\infty n(v) v dv = N_0 v_0 \quad (6)$$

Unfortunately, it is impossible to estimate  $f$  and  $N_0$  based solely on the results obtained from PAL spectroscopy. Instead we will use the following approach. Following Simha and Boyer<sup>42</sup> (see also van Krevelen<sup>43</sup>), the fractional free volume may be defined as the relative volume in an amorphous polymer being in excess to a hypothetical equilibrium volume  $V_0 = V_0(0)(1 + \alpha_g T)$ ,  $f = [V - V_0]/V$ , where  $V$  is the total (specific) volume at a temperature  $T$ .  $V_0(0)$  is the equilibrium volume of the amorphous polymer at 0 K which may be approximated by  $V_0(0) = 1.3 V_{\text{vdW}}$ , following Bondi.<sup>44</sup>  $V_0(0)$  is composed of the van der Waals volume  $V_{\text{vdW}}$  and the interstitial free volume. It expands, similarly to the glassy polymer,<sup>42,43</sup> approximately with the (cubic) coefficient of thermal expansion,  $\alpha_g$ . The fractional free volume at a temperature  $T$  may then be calculated from

$$f(T) = \frac{V(T) - V_0(T)}{V(T)} = \frac{V(T) - 1.3 V_{\text{vdW}}(1 + \alpha_g T)}{V(T)} \quad (7)$$

The molar mass of polyimide 6FDA-ODA is  $M = 606.4$  g/mol.<sup>43,44</sup> The mass density is influenced by the sample preparation method; we have determined a value of  $\rho = 1.43$  g/cm<sup>3</sup> for our polyimide PI2566 samples. Thus, the molar volume is  $V = M/\rho = 424.1$  cm<sup>3</sup>/mol. The van der Waals volume of the chemical repeating unit is calculated using Bondi's group contribution method, which yields  $V_{\text{vdW}} = 272.3$  cm<sup>3</sup>/mol.<sup>43,44</sup> Using  $\alpha_g = 2 \times 10^{-4}$  K<sup>-1</sup> in eq 6,<sup>45</sup> we obtain  $f = 0.115$ , and with  $v_0 = 0.134$  nm<sup>3</sup>, a number density of holes of  $N_0 = f/v_0 = 0.86$  nm<sup>-3</sup> is calculated. Values typically estimated for amorphous polymers<sup>37,46,47</sup> are between  $N_0 = 0.4$  and 1.3 nm<sup>-3</sup>.

When sorbed within a polymer, water molecules will first occupy only the larger of the local free volumes<sup>38,39</sup>—up to a limiting volume  $v_i$ .  $v_i$  depends on the number of sorbed (hole filling) water molecules  $N_i$  as follows:

$$N_i = \int_{v_i}^\infty n(v) dv \quad (8)$$

The mean volume of the holes not occupied by sorbed water may be calculated using

$$v_s = \frac{\int_0^{v_i} v n(v) dv}{N_s} \quad (9)$$

with

$$N_s = N_0 - N_i = \int_0^{v_i} n(v) dv \quad (10a)$$

and

$$N_0 = \int_0^\infty n(v) dv \quad (10b)$$

Ruling out a conceivable preference of the Ps probe for larger holes,<sup>39</sup>  $v_0$  may be associated with the mean hole volume estimated for the dry polyimide,  $v_0 = v_0(0)$ , while  $v_s$  corresponds to the mean volume of holes not filled with water molecules after water uptake,  $v_s = v_0(\text{RH})$ . This interpretation assumes that no Ps is formed or trapped in holes that are occupied by a water molecule.<sup>39</sup> The strong decrease of the o-Ps intensity  $I_3$  with increasing relative humidity may be considered as evidence for this model. It can be argued that the water molecule prevents the formation of Ps in a hole due to its polar nature.<sup>9</sup> From this we also conclude that the o-Ps intensity  $I_3$  directly mirrors the relative number of holes not occupied by water molecules:

$$I_3(\text{RH}) = c N_s \quad \text{with} \quad c = \frac{I_3(0)}{N_0} = 0.0605 \text{ nm}^3 \quad (11)$$

A linear dependence between the number of holes and the o-Ps intensity is indeed widely accepted in the literature.<sup>12,48</sup>

We have found that the sample preparation process has little impact on the o-Ps lifetime. All our dry polyimide PI2566 samples had nearly the same  $\tau_3$  values, regardless of whether they had been prepared by spin-coating or by casting. We therefore believe that it is justified to relate the free volume properties estimated from positron lifetime measurements on bulk samples with the results from our water uptake and swelling experiments on spin-coated polyimide films. We have also observed that the lifetime parameters are reversible; i.e.,  $\tau_3$  and  $I_3$  increase again when moist samples are dried. The number of sorbed water molecules may be estimated from the relative mass uptake of the polymer  $\Delta m_W/m_P$ , where  $\Delta m_W$  is the mass of the sorbed water vapor under steady-state conditions and  $m_P$  is the mass of the dry polymer. Figure 7 shows the relative mass uptake  $\Delta m_W/m_P$  and the volume expansion  $\Delta V/V$  due to the sorption of water in polyimide PI2566. As can be seen,  $\Delta m_W/m_P$  increases roughly linearly with relative humidity.<sup>49,50</sup> Only at larger humidity values does  $\Delta m_W/m_P$  increase faster than predicted by the linear dependence, which might be explained as the clustering of water molecules.<sup>50,51</sup>

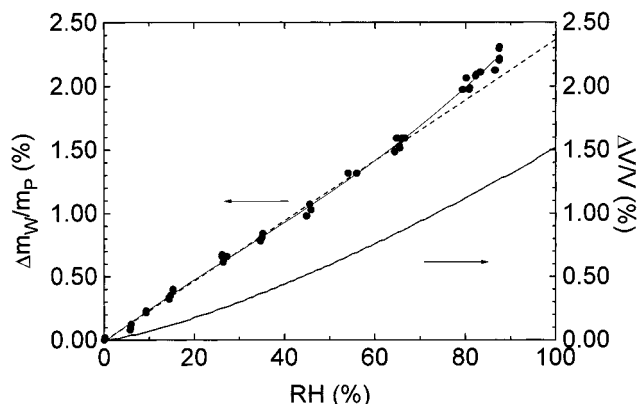


**Figure 7.** Relative (saturated) mass uptake  $\Delta m_W/m_P$  and volume expansion  $\Delta V/V$  of polyimide PI2566 as a function of RH. The solid line represents a fourth-order polynomial fit to the experimental  $\Delta m_W/m_P$  data. A straight dashed line is fitted to the data below RH = 70%.

The number density of sorbed water molecules,  $N_i$ , was calculated from the mass uptake  $\Delta m_W/m_P$ . To obtain a linear relationship between RH and  $N_i$ , we have linearized the  $\Delta m_W/m_P$  data from Figure 7 by least-squares fitting a straight line to all of the experimental data points. At 100% RH, this yields a maximum saturation mass uptake of 2.5%. The total volume of a water molecule (in the liquid phase) is calculated from  $v_W = [18 \text{ cm}^3/\text{mol}]/[6.02217 \times 10^{23} \text{ 1/mol}] = 0.0299 \text{ nm}^3$ , and its mass is  $m_W = [18.02 \text{ g/mol}]/[6.02217 \times 10^{23} \text{ 1/mol}] = 2.99 \times 10^{-23} \text{ g}$ .  $N_i$  is calculated using

$$N_i = \frac{(\Delta m_W/m_P)\rho_P}{m_W} \quad (12)$$

where  $\rho_P = 1.43 \text{ g/cm}^3$  is the mass density of polyimide PI2566. For a water uptake of  $\Delta m_W/m_P = 2.5\%$  at RH = 100%, we obtain  $N_i = 1.20 \times 10^{21} \text{ cm}^{-3} = 1.20 \text{ nm}^{-3}$ . Note that this value is only slightly larger than the number density of holes estimated previously.

The nature of the sorption process as detected by Ps is illustrated in Figure 8 where we have plotted the number density of empty holes,  $N_s$ , estimated using eq 11 from  $I_3$ , versus the number density of sorbed water molecules,  $N_i$ , estimated using eq 12. The dashed line indicates the theoretical dependence, with each of the  $N_i$  sorbed water molecules occupying a hole,  $N_s = N_0 - N_i$  (eqs 8 and 10),  $N_i = N_s$ . Evidently, this is indeed the case up to  $N_i \approx 0.4 \text{ nm}^{-3}$  (RH  $\approx 30\%$ ). For larger humidity values, hole filling proceeds somewhat slower, indicating that the fraction  $N_i - (N_0 - N_s) = N_i - N_i$  of sorbed water molecules now occupy sites other than the empty preexisting holes detected by the Ps probe. Such sites might be regular interstitial free volume regions (not preexisting holes), for example. In this case, swelling of the polymer, as observed in Figure 7, is expected.

Another explanation for the slower hole-filling process at larger humidity values is that it might be energetically more favorable for a water molecule to slide into a large hole already occupied by another water molecule, rather than find an empty, but smaller, hole. In fact, the mean size of holes not occupied by a water molecule decreases from  $0.134 \text{ nm}^3$  for RH = 0% to about  $0.105 \text{ nm}^3$  for RH = 50%. This decrease corresponds to the volume of a single water molecule, meaning that, on the average, the available space in the large holes already

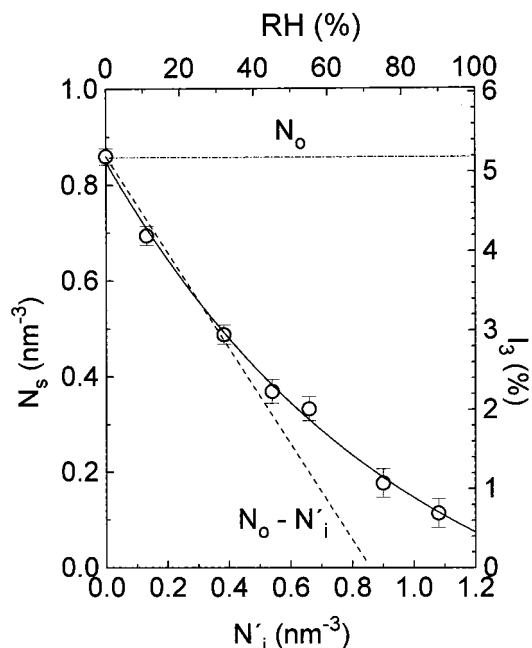


**Figure 8.** Number density of holes  $N_s$  not occupied by water molecules (estimated from  $I_3$  using eq 11) as a function of the number density  $N_i$  of water molecules sorbed at a relative humidity RH (estimated from eq 12).  $N_0$  is the total number density of holes estimated from eqs 6 and 7.

occupied by a water molecule now exceeds the volume of the small, empty holes. To provide a quantitative comparison, we note that the number of empty holes with volume  $v < v_i$  decreases with  $N_s(v_i)$  as  $N_i$  increases (see eq 10), while the number of already occupied holes with available space  $v > v_i - v_W$  increases with  $N_0 - N_s(v_i + v_W)$ . The ratio  $N_s(v_i)/[N_0 - N_s(v_i + v_W)]$  has a value of only 0.3 at RH = 50%, but a value of 6 at RH = 90%. Although the quantitative relationships discussed in Figure 8 depend strongly on the accuracy in estimating  $N_0$ ,  $N_s$ , and  $N_i$ , the fact that the slope in the experimental  $N_s$  declines with increasing  $N_i$  clearly indicates a deviation from the simple hole-filling model at larger numbers of sorbed water molecules.

Multiple occupation of large holes might be considered an early stage of water cluster formation. In Figure 9 we have plotted the fractional number of "excess" water molecules ( $N_i/N_i - 1$ ) as a function of the relative humidity together with the composition parameter  $\Phi_1 G_{11}/v_1$ , estimated from the mass uptake curve following Zimm and Lundberg.<sup>50,51</sup> The composition parameter  $\Phi_1 G_{11}/v_1$  is equal to the "average number of penetrant molecules in the neighborhood of a given penetrant molecule in excess of the mean (ideal solution) concentration".<sup>50,51</sup> Due to the convex curvature in the  $\Delta m_W/m_P$  isotherm, the composition parameter  $\Phi_1 G_{11}/v_1$  is larger than zero for RH  $\geq 30\%$ , which indicates clustering of water molecules. (For details of calculation of  $\Phi_1 G_{11}/v_1$  see refs 50 and 51.) Assuming that  $N_i > N_i$  is due to multiple occupation of holes, the quantity  $(N_i/N_i - 1)$  corresponds to the case where the mean number of water molecules per hole exceeds 1. Considering that  $\Phi_1 G_{11}/v_1$  and  $(N_i/N_i - 1)$  were estimated using different approaches, the correlation between the two quantities observed in Figure 9 is satisfactory.

From the volume expansion of the polyimide,  $\Delta V$ , and the number of sorbed water molecules,  $N_i$ , one can estimate the partial molar volume of water,  $v_P = \Delta V/N_i$ .  $v_P$  increases with relative humidity and saturates

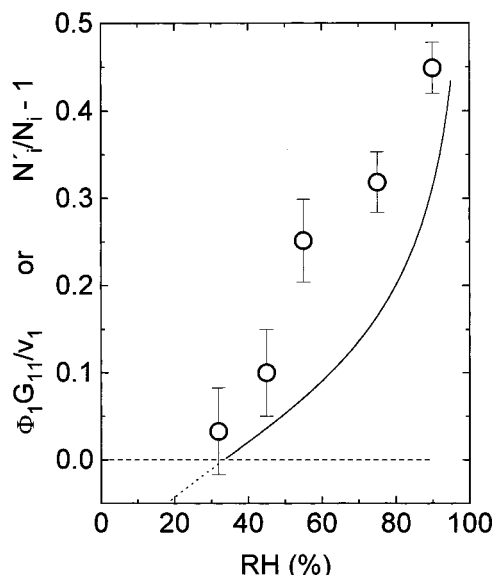


**Figure 9.** Zimm-Lundberg composition parameter,  $\Phi_1 G_{11}/N_1$  (solid line) and fractional number of "excess" water molecules  $N_i/N_i - 1$  (empty circles, see text) as a function of relative humidity RH.

at a value of  $v_p = 0.011 \text{ nm}^3$ . The experimental finding that  $v_p > 0$  is surprising taking into account the large size of the holes in polyimide ( $v_0 \approx 4 v_w$ ). Although the nature of this discrepancy is still unclear, we shall list a number of possible explanations: (i) the nonspherical shape of the water molecule, coupled with the anisotropy of free volume holes; (ii) the increase in the momentum of the water molecule due to its confinement in holes; and (iii) a possible plasticization at the sorption sites. Hydrogen bonding of the water molecules to C=O groups within the polyimide can be expected to cause the polymer to expand.<sup>52</sup> Plasticization at sorption sites in gas-exposed polymers was observed recently by Ito et al.,<sup>53</sup> Hong et al.,<sup>54</sup> and Bohlen et al.<sup>39</sup> using PAL experiments.

**Hole Size Distribution.** The mean size  $v_s$  of holes not occupied by water molecules depends on the fractional number of occupied holes,  $N_i/N_0$ . The  $v_s$  versus  $N_i/N_0$  function is controlled by the mean size  $v_0$  and the width  $\sigma_0$  of the original hole size distribution. Since  $v_0$  is known, this relation may be used to estimate  $\sigma_0$ . In Figure 10 we plot the experimental mean hole volume  $v_s = v_0(\text{RH})$ , which was estimated from the o-Ps lifetime  $\tau_3$  extrapolated to  $t_M \rightarrow 0$ , as a function of the fractional occupation of holes,  $N_i/N_0 = (N_0 - N_s)/N_0 = [I_3(0) - I_3(\text{RH})]/I_3(0)$ . We can compare this behavior with the model distribution described by eq 5, assuming  $v_0(0) = v_0 = 0.134 \text{ nm}^3$ , as determined for the dry polyimide PI2566, and using the width  $\sigma_0$  as a fitting parameter.  $v_s$  was calculated using eq 9, and  $N_i$  was determined using eq 8. Model and experiment agree well for  $\sigma_0 = 0.030 \pm 0.005 \text{ nm}^3$  (Figure 10). PAL experiments on polycarbonate and polystyrene show that ratios of  $\sigma_0/v_0 \approx 0.2$  are typical for glassy polymers.<sup>28</sup>

As can be seen in Figure 2, the o-Ps lifetime peak in polyimide PI2566 when exposed to RH = 90% is distinctly narrower than that for RH = 0%. This may indicate a decrease in the effective width of the part of the holes size distribution describing unoccupied holes. From the analysis of computer-generated spectra we have found, however, that as a result of the decreasing sensitivity of the MELT routine, the width of the

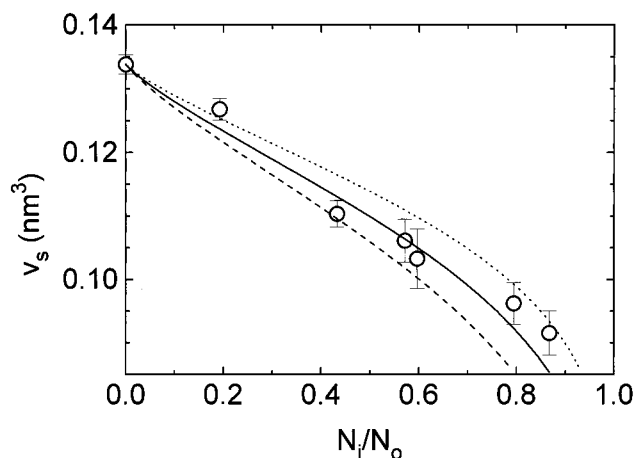


**Figure 10.** Mean volume  $v_s$  of holes not occupied by water molecules as a function of the fraction of holes occupied by water molecules,  $N_i/N_0$ : empty circles, experimental values estimated from  $\tau_3$  using eq 4; lines, values calculated using eq 9 assuming a mean hole volume of  $v_0 = 0.134 \text{ nm}^3$  and a standard deviation  $\sigma_0$  of the hole size distribution in eq 5 of  $0.025 \text{ nm}^3$  (dashed line),  $0.030 \text{ nm}^3$  (solid line), and  $0.035 \text{ nm}^3$  (dotted line).

analyzed distribution decreases with decreasing o-Ps intensity  $I_3$ . Thus, at least part of the observed decrease in peak width is a computational artifact due to the decrease in  $I_3$ . Nevertheless, part of the decrease does seem to have a physical meaning, at least qualitatively.

## Conclusions

When polyimide 6FDA-ODA (PI2566) is exposed to atmospheres of controlled relative humidity, the material shows increasing mass uptake from RH = 0% to 100%, with a maximum mass uptake of 2.5% at RH = 100%. PAL measurements indicate a decrease in o-Ps lifetime  $\tau_3$  from 2375 to 1925 ps and a decrease in intensity  $I_3$  from 5.2% to 0.7% when RH varies between 0% and 90%. The mean volume of holes can be estimated from  $\tau_3$  and their number density from  $I_3$ . Experimental data were analyzed under the following assumptions: (i) a Gaussian size distribution of pre-existing (excess free volume) holes, (ii) o-Ps occupies all (empty) holes with the same probability, and (iii) the holes occupied by at least one water molecule are not sensed by the o-Ps probe.

Under these assumptions a mean hole volume of  $v_0 = 0.134 \text{ nm}^3$ , a hole number density of  $N_0 = 0.86 \text{ nm}^{-3}$  (from a comparison of  $v_0$  with the fractional Bondi free volume,  $f = v_0 N_0 = 0.115$ ), and a standard deviation of  $\sigma_0 = 0.030 \text{ nm}^3$  for the (original) hole size distribution were estimated from PAL spectra of dry polyimide PI2566. The PAL data are consistent with a model according to which the early and medium stages of water sorption are dominated by the occupation of large holes—each by a single water molecule. Above about RH  $\approx 30\%$  an increasing fraction of sorbed water molecules occupies sites other than empty preexisting holes, and multiple occupation of large holes appears to be a possible mechanism. The behavior of the fractional number of "excess" water molecules agrees well with the composition parameter estimated from the mass uptake by applying the clustering theory of Zimm and Lundberg.

A solution of water molecules into interstitial free volume regions, however, would also explain the appearance of "excess" water molecules in the positron



lifetime data. The observed increase in the partial molar volume of water,  $v_p$ , with relative humidity (saturation value of  $v_p = 0.011 \text{ nm}^3$ ) seems to contradict the simple hole-filling model. As a result of the large mean hole size,  $v_p = 0$  would be expected during this particular stage of sorption. We have presented and discussed possible explanations for the observed discrepancy.

**Acknowledgment.** The authors thank P. Hautajärvi (Helsinki) and A. Shukla (Geneva) for supplying the PC versions of the routines LIFSPECFIT and MELT. S. Eichler (Halle) is acknowledged for making available the routine for simulating lifetime spectra. Furthermore, we gratefully acknowledge financial support from the German Bundesministerium für Bildung, Wissenschaft, Forschung und Technologie BMBF (Grant 16SV248-0) and from the Stiftung Industrieforschung (Grant T 48/96). In addition, the authors thank K. Baumann from AKTIV SENSOR GmbH for sample preparation.

## References and Notes

- (1) Sroog, C. E. *Polyimides*; Pergamon Press: Oxford, 1991.
- (2) Ghosh, K.; Mittal, K. L. *Polyimides, Fundamentals and Application*; Marcel Dekker: New York, 1996.
- (3) Okamoto, K. Sorption and Diffusion of Water in Polyimide Films. In ref 2, p 265.
- (4) Van Alsten, J. G.; Coburn, J. C. *Macromolecules* **1994**, *26*, 3746 and references therein.
- (5) Dupasquier, A.; Mills, Jr., A. T., Eds. *Positron Spectroscopy of Solids, Proc. Int. School "Enrico Fermi"*, Varenna, Italy, July 1993; IOS Press: Amsterdam, 1995.
- (6) Kajcsos, Zs.; Levay, B.; Süvegh, K., Eds. 5th International Workshop on Positron and Positronium Chemistry (ppc 5), Lillafüred, Hungary, June 1996. *J. Radioanal. Nucl. Chem.* **1996**, *210* (2), 255–642; **1996**, *211* (1), 1–282.
- (7) Jean, Y. C.; Eldrup, M.; Schrader, D. M.; West, R. N., Eds. *Positron Annihilation; Proc. of the 11th Int. Conf., ICPA11*, Kansas City, MO, May 1997; *Mater. Sci. Forum* **1998**, 255–257.
- (8) Pethrick, R. A. *Prog. Polym. Sci.* **1997**, *22*, 1.
- (9) Mogensen, O. E. *Positron Annihilation in Chemistry*; Springer-Verlag: Heidelberg, 1995.
- (10) Eldrup, M.; Lightbody, D.; Sherwood, J. N. *Chem. Phys.* **1981**, *63*, 51.
- (11) Nakanishi, H.; Jean, Y. C. In *Positron and Positronium Chemistry, studies in physical and theoretical chemistry 57*; Schrader, D. M., Jean, Y. C., Eds.; Elsevier Sci. Publ.: Amsterdam, 1988; p 159.
- (12) Jean, Y. C. *Microchem. J.* **1990**, *42*, 72. Jean, Y. C. In *Positron Annihilation; Proc. 10th Int. Conf.*, He, Y. J., Cao, B.-S., Jean, Y. C., Eds. *Mater. Sci. Forum* 175–178, Trans Technol. Publ.: 1995; p 59.
- (13) Jean, Y. C.; Sandreczki, T. C.; Ames, D. P. *J. Polym. Sci., Part B: Polym. Phys.* **1986**, *24*, 1248.
- (14) Eftekhari, A.; Chlair, A. K. St.; Stoakley, D. M.; Kuppa, S.; Singh, J. J. *J. Polym. Mater. Sci. Eng.* **1992**, *66*, 279.
- (15) Okamoto, K.; Tanaka, K.; Katsube, N.; Sueoka, O.; Ito, Y. In *Positron Annihilation; Proc. 9th Int. Conf.*, Kajcsos, Z., Szeles, C. Eds.; *Mater. Sci. Forum* **1992**, 105–110, 1675.
- (16) Ito, Y.; Okamoto, K.-I.; Tanaka, K. In *4th Int. Workshop on Positron and Positronium Chemistry* (ppc 4), Le Mont Sainte-Odile, France, June 1993, Billard, I., Ed.; *J. Phys. IV* **1993**, *3*, Colloq. C4, Suppl. II, No. 9, 241.
- (17) Ito, Y. In *Positron Annihilation, Proc. of the 10th Int. Conf.*, He, Y. J., Cao, B.-S., Jean, Y. C., Eds.; *Mater. Sci. Forum* **1995**, 175–178, Trans Technol. Publ., p 627.
- (18) Tanaka, T.; Ito, M.; Kita, H.; Okamoto, K.; Ito, Y. In *Positron Annihilation*; He, Y. J., Cao, B.-S., Jean, Y. C., Eds.; *Mater. Sci. Forum* **1995**, 175–178, Trans Technol. Publ., p 789.
- (19) Jean, Y. C.; Yuan, J. P.; Liu, J.; Deng, Q.; Yang, H. *J. Polym. Sci., Part B: Polym. Phys.* **1995**, *33*, 2365.
- (20) Doveck, J. Y.; Dai, G. H.; Moser, P.; Pineri, M.; Aldebert, P.; Escoubes, M.; Avrillon, R.; Mileo, J. C. *Positron Annihilation, Proc. 9th Int. Conf.*, Kajcsos, Z.; Szeles, C. Eds.; *Mater. Sci. Forum* **1992**, 105–110, 1549.
- (21) Baugher, A. H.; Kossler, W. J.; Petzinger, K. G.; Pater, R. H. In Jean, Y. C., Eldrup, M., Schrader, D. M., West, R. N., Eds. *Positron Annihilation, Proc. of the 11th Int. Conf., ICPA11*, Kansas City, MO, May 1997; *Mater. Sci. Forum* **1998**, 57.
- (22) LIFSPECFIT 5.1, Lifetime spectrum fit version 5.1, Technical University of Helsinki, Laboratory of Physics, 1992.
- (23) Shukla, A.; Peter, M.; Hoffmann, L. *Nucl. Instrum. Methods* **1993**, *A335*, 310. Hoffmann, L.; Shukla, A.; Peter, M.; Barbiellini, B.; Manuel, A. A. *Nucl. Instrum. Methods* **1993**, *A335*, 276.
- (24) Buchhold, R.; Nakladal, A.; Sager, K.; Gerlach, G.; Sahre, K.; Müller, M.; Eichhorn, K.-J.; Herold, M.; Gauglitz, G. *Proceedings of The Materials Research Society Spring Meeting*, San Francisco, 1998; Vol. 511, p 359.
- (25) Buchhold, R.; Nakladal, A.; Sager, K.; Gerlach, G.; Sahre, K.; Müller, M.; Eichhorn, K.-J.; Herold, M.; Gauglitz, G. *J. Electrochem. Soc.* **1998**, *145*, 4012.
- (26) Franke, H.; Wagner, D.; Kleckers, T. *Appl. Opt.* **1993**, *32* (16), 2927.
- (27) Gregory, R. B.; Zhu, Y. *Nucl. Instrum. Methods* **1990**, *A290*, 172.
- (28) Dlubek, G.; Hübner, Ch.; Eichler, S. *Nucl. Instrum. Methods B* **1998**, *142*, 191. Dlubek, G.; Eichler, S. *Phys. Status Solidi A* **1998**, *168*, 333. Dlubek, G.; Eichler, S.; Hübner, Ch.; Nagel, Ch. *Nucl. Instrum. Methods B*, in press.
- (29) Bertolaccini, M.; Bisi, A.; Gambarini, G.; Zappa, L. *J. Phys.* **1974**, *C7*, 3827.
- (30) Consolati, G. *J. Radioanal. Nucl. Chem.* **1996**, *210* (2), 27.
- (31) Vleeshouwers, S.; Kluin, J.-E.; McGervey, J. D.; Jamieson, A. M.; Simha, R. *J. Polym. Sci., Part B: Polym. Phys.* **1992**, *30*, 1429.
- (32) Kluin, J. E.; Yu, Z.; Vleeshouwers, S.; McGervey, J. D.; Jamieson, A. M.; Simha, R.; Sommer, K. *Macromolecules* **1993**, *26*, 1853.
- (33) Deng, Q.; Sundar, C. S.; Jean, Y. C. *J. Phys. Chem.* **1992**, *96*, 807.
- (34) Okamoto, K.; Tanihara, N.; Watanabe, H.; Tanaka, K.; Kita, H.; Nakamura, A.; Kusuki, Y.; Nakagawa, K. *J. Polym. Sci., Part B: Polym. Phys.* **1992**, *30*, 1223.
- (35) Lim, B. S.; Nowick, A. S.; Lee, K.-W.; Viehbeck, A. *J. Polym. Sci., Part B: Polym. Phys.* **1993**, *31*, 545.
- (36) Tao, S. J. *J. Chem. Phys.* **1972**, *56*, 5499.
- (37) Liu, J.; Deng, Q.; Jean, Y. C. *Macromolecules* **1993**, *26*, 7149.
- (38) Kirchheim, R. *J. Polym. Sci., Part B: Polym. Phys.* **1993**, *31*, 1373.
- (39) Bohlen, J.; Wolff, J.; Kirchheim, R. In Jean, Y. C., Eldrup, M., Schrader, D. M., West, R. N., Eds. *Positron Annihilation, Proc. of the 11th Int. Conf., ICPA11*, Kansas City, MO, May 1997; *Mater. Sci. Forum* **1998**, 393.
- (40) Jordan, S. S.; Koros, W. J. *Macromolecules* **1995**, *28*, 2228.
- (41) Bueche, F. *J. Chem. Phys.* **1953**, *21*, 1850.
- (42) Simha, R.; Boyer, R. F. *J. Chem. Phys.* **1962**, *37*, 1003.
- (43) Van Krevelen, D. W. *Properties of Polymers*; Elsevier Sci. Publ. Co.: Amsterdam, 1990.
- (44) Bondi, A. *J. Phys. Chem.* **1964**, *68*, 441. Bondi, A. *Physical Properties of Molecular Crystals, Liquids, and Gases*; Wiley: New York, 1968; p 450.
- (45) Coburn, J. C.; Pottiger, M. T.; Pryde, C. A. *Mater. Res. Symp. Proc.* **1993**, *308*, 475.
- (46) Dlubek, G.; Saarinen, K.; Fretwell, H. M. *J. Polym. Sci., Part B: Polym. Phys.* **1998**, *36*, 1513.
- (47) Dlubek, G.; Stejny, J.; Alam, M. A. *Macromolecules* **1998**, *31*, 4574.
- (48) Kobayashi, Y.; Haraya, K.; Hattori, S.; Sasuga, T. *Polymer* **1994**, *35*, 925.
- (49) Vieht, W. R.; Howell, J. M.; Hsieh, J. H. *J. Membr. Sci.* **1976**, *1*, 177.
- (50) Zimm, B. H.; Lundberg, J. L. *J. Phys. Chem.* **1956**, *60*, 425.
- (51) Lundberg, J. L. *J. Macromol. Sci. Phys.* **1969**, *B3* (4), 693.
- (52) Schere, J. R.; Bolton, B. A. *J. Phys. Chem.* **1985**, *89*, 3535.
- (53) Ito, Y.; Mohamed, H. F.; Tanaky, K.; Okamoto, K.; Lee, K. *J. Radioanal. Nucl. Chem.* **1996**, *211* (1), 211.
- (54) Hong, X.; Jean, Y. C.; Hsinjin Yang; Jordan, S. S.; Koros, W. J. *Macromolecules* **1996**, *29*, 7859.